Doctor of Philosophy

Biocompatibility and Efficiency of Biodegradable Magnesium-Based Plates and Screws in the Mandible Fracture Model of Beagles

The Graduate School

of the University of Ulsan

Department of Medicine

Hong, JunHee

Biocompatibility and Efficiency of Biodegradable Magnesium-Based Plates and Screws in the Mandible Fracture Model of Beagles

Supervisor : Lee, Bu-Kyu

A dissertation

Submitted to the Graduate School of the University of Ulsan

In partial Fulfillment of the Requirements

for the Degree of

Doctor of philosophy

by

Hong, JunHee

Department of Medicine

Ulsan, Korea

December 2018

Biocompatibility and Efficiency of Biodegradable Magnesium-Based Plates and Screws in the Mandible Fracture Model of Beagles

This certifies that the dissertation of Hong, Jun-Hee is approved.

Hwang, Chang-Mo

Committee Chair Dr.

Lee, Bu-Kyu

Committee Member Dr.

Kim, Byung-Soo

Committee Member Dr.

Kim, Yu-Chan

Committee Member Dr.

Park, Sang-Hyuk

Committee Member Dr.

Department of Medicine

Ulsan, Korea

December 2018

Biocompatibility and Efficiency of Biodegradable Magnesium-Based Plates and Screws in the Mandible Fracture Model of Beagles

JunHee Hong, D.D.S, M.S.D.

Directed by Bu-Kyu Lee, D.D.S., M.S.D., Ph.D

Departmant of Dentistry, Graduate school of Medicine, University of Ulsan

Background

Trauma involving bone are very common and occur six million bone fracture each year in the United States. These fractures are caused by a variety of causes such as birth defect, osteoporosis, osteomyelitis, MRONJ (Medication related osteonecrosis of the jaw) and, most commonly, trauma. As the population ages and the number of medically compromised patients increases, the rate of pathologic bone fracture is expected to be increased in the future. For this reason, fracture treatment remains an important clinical focus in bone tissue engineering. Fracture treatments often require internal fixation. Plates and screws are used for alignment and stabilization of bone fragments. Largely, two kind of internal bone fixation devices have been used such as metallic and polymeric substances. Internal anchors made of permanent metal are associated with numerous long-term complications and may require removal. Polymeric materials are biodegradable and need not be removed, but are known to have poorer mechanical quality than metals.

Unlike permanent metals and resorbable polymers, degradable magnesium alloys can provide an ideal balance of degradation and strength. Recent investigations of magnesium alloys in vivo have highlighted their potential as bone fixation materials.

Purpose

A biodegradable magnesium alloy system has been developed as a substitute for conventional plates and screws made of titanium or absorbable polymer. However, previous studies were limited to small animal experiments using screws or wires. In this study, human standard-sized degradable magnesium devices were evaluated by using the mandible fracture model of beagles. Device degradation, fracture healing, and new bone formation were assessed.

Method and Materials

The biodegradable magnesium alloy plate products are evaluated using biological safety / efficacy in large animals. Among large animals, beagle, in which the masticatory and oral conditions are similar to those of humans, is routinely selected as an experiment related to CMF implants and other dental materials. The hydrogen gas generation and decomposition behavior around the plates were evaluated for the fracture site on the mandibular right mandible. Micro CT images were performed 5 times at 4 weeks interval (1, 4, 8, 12, 16 weeks) immediately after implantation. Bone and tissue volumes were calculated using CT analyzing software. Histology was performed after sacrifice. Local response and biocompatibility were evaluated.

Result

The biodegradable magnesium plates used in this study were found to be a positive result in histological and pre-clinical evaluation after 16 weeks of CT and after sacrifice. Particularly, additional bone formation in the surgery site was found when it compared to the control site, and hydrogen gas pocket

formation as a result of plate decomposition was observed in one animal. However, all dogs underwent normal healing process. Further study is recommended to confirm that bone deposition is more prevalent in comparison with the control site before the prototype is applied to humans, and how to control hydrogen production at the early stage of surgery.

Key words : absorbable plate, magnesium plate, beagle, biocompatibility.

List of table

List of figure

Index

Introduction

The goal of modern medicine is to keep human being healthy by providing normal physical function and mental wellness. What makes dentistry unique is the ability to supporting this goal by maintaining healthy oral condition, providing proper masticatory, swallowing, phonetic function, regardless of the age-related atrophy, disease, or traumatic injury of the stomatognathic system. Aging often makes man medically and dentally compromised. Old men who needs to be assisted by appropriate medical and dental aids are called patients. Furthermore, according to the literature, age is directly related to every indicator of tooth loss. [1)] Therefore the aging population is an important factor to consider in dentistry. Old people tends to have less teeth and thinner atrophic alveolar bone than young people. The density and thickness of the alveolar bone is directly related to its strength. So, it can be fractured more easily when it was subjected then same amount of impact. Furthermore, the more teeth a patient is missing, the more challenging to make a good oral function by proper surgical mean. [2)]

As the number of medically and dentally compromised old people increases, prevalence of osteoporosis, osteomyelitis, MRONJ (Medication related osteonecrosis of the jaw) and incidence of pathologic bone fracture are expected to rise within the next few years. Furthermore, not only in old people, but also in young and healthy people, traumatic bone fracture always can be happened. In fact, trauma involving bone are very common and occur six million bone fracture each year in the United States.[3)] For this reason, fracture treatment is still an important clinical focus within the bone tissue engineering field.

Fracture treatments often require internal fixation. Plates and screws were

incorporated for the proper alignment and stabilization of separated bone fragments. Conventionally, metallic materials have continued to play a vital role in surgical repair when bone tissue was damaged. Titanium alloy was typically utilized since it's character is mechanically proper, bio-inert and non-degradable.[4] This metal was initially chosen for strength and biocompatibility but has been shown to cause long-term complications such as inhibition of pediatric skeletal growth, pain, tissue irritation, metallosis, infections, debris accumulation in the liver and kidneys, local inflammation and necrosis of surrounding bony structure.[5] To avoid these complications, a second surgical procedure can be used to remove the device but it increases total surgical risk, treatment time and costs.[6]

There have been many biodegradable appliances which were composed of polymeric substances. Absorbable plates are composed of macromolecular chains which form a single polymer. Polymers used in absorbent plates include polylactic acid, polyglycolic acid, polyglyconate and polydioxanone. Among these, polylactic acid and polyglycolic acid are the most widely used. Polyglycolic acid is absorbed within a month and is a crystalline polymer with considerable flexural strength. Polylactic acid has two isomeric configurations, poly-L-lactic acid (PLLA) and poly-DL-lactic acid (PDLLA). Of the two isomers, absorbable plates made from PLLA have greater strength but takes five to six years for absorption. In contrast, PDLLA is mechanically less rigid but is resorbs within a year. For example, unsintered hydroxyapatite/PLLA plate system OSTEOTRANS MX® (Takiron Co., Ltd., Osaka, Japan) is currently used in craniomaxillofacial surgery to avoid the second surgery for the removal of plate. [7] Today, absorbable plates are made with varying ratios of PLLA and PDLLA or PDLLA and polyglycolic acid, to meet mechanically acceptable criteria which are absorbed within nine months to three years.[8] (Table 1) However, its strength is not considered to

be sufficient. Many surgeons still hesitate to use this system in mechanically demanding area.

Table 1. Commercially available resorbable plating system.

Product (manufacturer)	Polymer composition (%)	Resorption
LactoSorb (W. Lerenz Surgical Inc.)	PLLA (82); PGA (18)	6–12 M
Macropore (Medtronic)	PLLA (70); PDLLA (30)	1–3 Y
Bionx (Bionx Implants Inc.)	PLLA (70); PDLLA (30)	1–2 Y
Resorbable Fixation System (Synthes)	PLLA (70); PDLLA (30)	1–6 Y
DeltaSystem (Stryker-Leibinger)	PLLA (85); PDLLA (5); PGA (10)	1.5–3 Y
Inion CPS (Inion)	PLLA; PDLLA; TMC	1–2 Y
Osteotrans MX (Takiron)	HA (70) PLLA (30)	1–2 Y

PLLA, poly-L-lactic acid; PGA, poly glycolic acid; PDLLA, poly-DL-lactic acid; TMC, trimethylene carbonate; HA, hydroxyapatite.

Y : year, M : month

Hydroxyapatite (HA) is bioabsorbable synthetic ceramic material and is widely used as substitute of bones in many medical fields including orthopedic surgery, neurosurgery and CMF surgery. [9-11] β-tricalciumphosphate (β-TCP) is also bioabsorbable and is commonly utilized synthetic ceramic material. [12] HA and β-TCP are main component to be mixed proportionately for bone substitutes in many synthetic bone graft material. [13] For example, Frabone (Inobone, Korea) is frequently used synthetic bone graft material in implant dentistry. It is composed 60% of HA and 40% of β-TCP. Today, many synthetic and xenographic, which means across-species including bovine, porcine, and equine source, dental bone graft materials are commercially available. Also, there is one company developed commercial allographic bone material. (Table 2) Its biocompatibility and bone regeneration ability will be discussed comparatively with other materials utilizing various growth factor in later part of this study.

Table 2. Commercially available dental bone graft materials.

Product (manufacturer)	material source and composition (%)	Resorption
Frabone (Inobone)	HA (60); β-TCP (40)	1-3 Y
Bio-oss (Geistlich)	Bovine bone (100)	1-2 Y
Infuse Bone Graft (Medtronics)	Bovine collagen (100); rh-BMP2 (1.5 mg/mL)	1-2 M
Bone-D (Medpark)	Porcine bone (100)	1-2 Y
Equimatrix (Nibec)	Equine Bone (100)	1-2 Y
BMP plus kit (Cowellmedi)	HA (30); β-TCP (70); rh-BMP2	6-12 M
OP-1 putty (Stryker)	Bovine collagen, Carboxymethylcellulose sodium; rh-BMP7; OP-1	1-2 M
Rafugen BMP2 (Cellumed)	Human bone (100); rh-BMP2 (50 ug/mL)	6-12 M

HA, Hydroxyapatite; β-TCP, β-tricalciumphosphate; rh-BMP, recombinant human - bone morphogenic protein; OP-1, osteogenic protein.

Y : year, M : month

When it comes to the biodegradable fixation plates, it is reported that polymeric composites with ceramic contents ranging between 70 and 85 wt.% have mechanical properties that match reasonably those of human cortical bone.[14] Additionally, a study about magnesium plates coated with HA to maintain mechanical strength, increase biocompatibility, and control biodegradation rate in body fluid was published recently.[15]

Over the past decade, magnesium and its alloys are considerably attracted attention as biomedical degradable implants, such as orthopedic and vascular stents.[4,16,17] Since magnesium alloys dissolve readily in aqueous solution especially that contains chloride ion, biomaterial researchers have developed them as a new kind of biodegradable material. [18,19] In this point of view, magnesium alloys have three major advantages over traditional materials such as stainless steel and titanium. Firstly, when magnesium alloys used in orthopedic surgery instead of stainless steel and titanium, a second surgery to remove the foreign material is unnecessary after the bone tissue has healed well. Secondly, Mg is an essential macro-element in human body. For a normal adult, daily intake of Mg is estimated to be about 400 mg, and excessive Mg can be excreted through the urine effectively.[20,21] Finally, Mg ion in the body has an ability to facilitate the mineral apposition rate and osteoblastic activity. It significantly stimulates the growth of new bone tissues, promoting bone healing. [16] However, there have been only a few studies of magnesium alloys in the area of craniomaxillofacial surgery. [22]

Material and methods

The study was undertaken with the support of the Asan Institute for Life Sciences in the Asan Medical Center, Seoul, South Korea.

The biodegradable magnesium plate and screws were provided by the Korean Institute of Science and Technology (KIST), Seoul, South Korea. In the present study, the biodegradable craniomaxillofacial (CMF) plate and screws are evaluated using biological safety / efficacy. Numerous in vitro and in vivo studies have demonstrated the biocompatibility and osteoconductivity of these materials. In vivo studies assessing Mg implants in endosseous sites, such as guinea pig, drat, and rabbit have conducted. [22-26] However, there was no study on dog. Among large animals, Beagles, in which the masticatory and oral conditions were similar those of humans, were routinely selected as an experiment related to CMF implants and other dental materials. [27-29]

1. *In vivo* animal model

The present *in vivo* animal study was conducted in accordance with international standards on animal welfare[30] and was approved by the Animal Research Committee of the Asan Institute for Life Sciences. Six mature beagle dogs (weight: 13-15kg) were selected as an experimental model. The experiments were initiated three times in the same manner, and in each experiment two dogs underwent surgery.

Table 3. Date of initiation and sacrifice of beagles.

Beagle ID	Date of Initiation	Date of Sacrifice	*In vivo* period
1	2016.10.04.	2019.10.04.	3Y (scheduled)
2	2016.10.04.	2019.10.04.	3Y (scheduled)
3	2016.12.06	2017.04.25.	5M
4	2016.12.06	2017.04.25	5M
5	2017.05.23	2018.09.14	1Y 4M
6	2017.05.23	2018.09.14	1Y 4M

Y : year, M : month

General anesthesia was administered by a veterinary surgeon. Dogs were premedicated 30 minutes before surgery with acepromazine maleate BP (ACP, C-Vet Ltd, Bury St Edmunds, England; 0.15 mg/kg), given subcutaneously in the dorsal aspect of the neck. Intravenous pentobarbitone sodium (Sagatal, RMB Animal Health Ltd, Dagenham, England; 0.44 mg/kg) was administered through the cephalic vein on induction, and an oro-endotracheal tube was inserted. Anesthesia was maintained with halothane, oxygen, and nitrous oxide. Vital signs were monitored throughout the procedure.

Longitudinal incisions (length: ~40mm) was made below the right mandible, which was further exposed by dissection of the subcutaneous tissues to the periosteum. The mandible was osteotomized using an oscillating saw, resulting in mandibular bone fracture starting from the proximal mandible to the gingiva. Then, 25-mm & 4-hole biodegradable magnesium plate with bridge design, was inserted in right mandibular body and four 5-mm long screws were used to anchor as shown in figure 1. Subsequently, the incision was rinsed using 0.9% saline solution and sutured carefully. All these surgical procedures were performed under sterile conditions. Within 5d following the surgery, the beagle dogs were given an intramuscular injection of penicillin (8×10^5 units, twice per day).

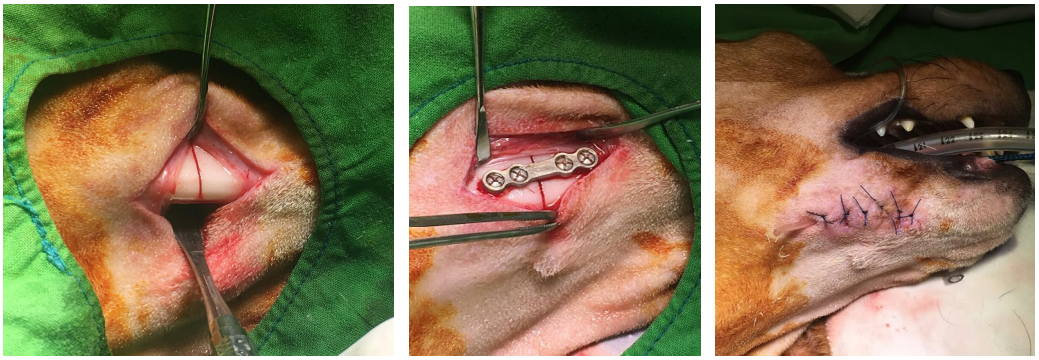

(a) (b) (c)

Figure 1. The mandibular bone fracture model prepared in the beagle dog and internal fixation using biodegradable magnesium plate.

2. Pre-clinical evaluation

Postoperatively, wound area in the right mandible of beagles were dressed and followed up.

3. Radiographical evaluation

CT imagings were performed 5 times at 4 weeks interval (1, 4, 8, 12, 16 weeks) immediately after implantation. High-resolution CT systems (Somatom Sensation 16, Siemens, Erlangen, Germany) were obtained to monitor device fixation and fracture healing. Two-dimensional slices and 3-dimensional reconstructions were created to evaluate fracture healing, device degradation, and new bone formation.

Animals were sacrificed after various intervals as described in Table 1., and their mandibles were extracted and scanned using micro-computed tomography (microCT) (SkyScan 1176; SkyScan, Kontich, Belgium). Scans were performed with an x-ray voltage of 50 kV, anode current of 500 uA, and image pixel size of 35.76 um. MicroCT analysis was performed using CT analyzing software (CT-Analyser, ver 1.16.4, SkyScan, Kontich, Belgium). We obtained tissue volume of mandibular bony segment including two premolars and one molar tooth by defining regions of interest (ROI) as shown in Figure 2. Except beagle No. 5 in which the microCT imaging was not processed in the same orientation on both sides, we made the right and left images under the same orientation. Then, CT analyzing software calculated bone volume through Otsu's algorithm. [31] (Figure 2. and 3.)

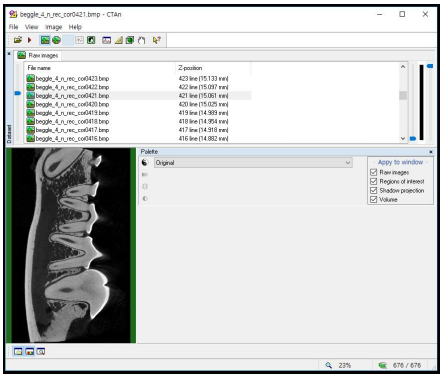

(a)

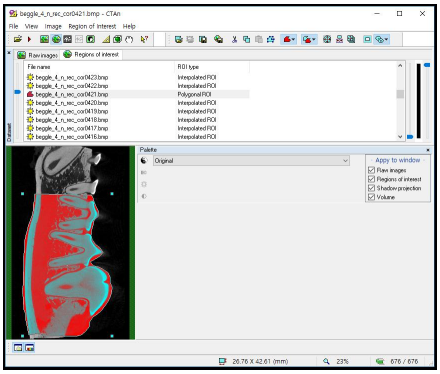

(b)

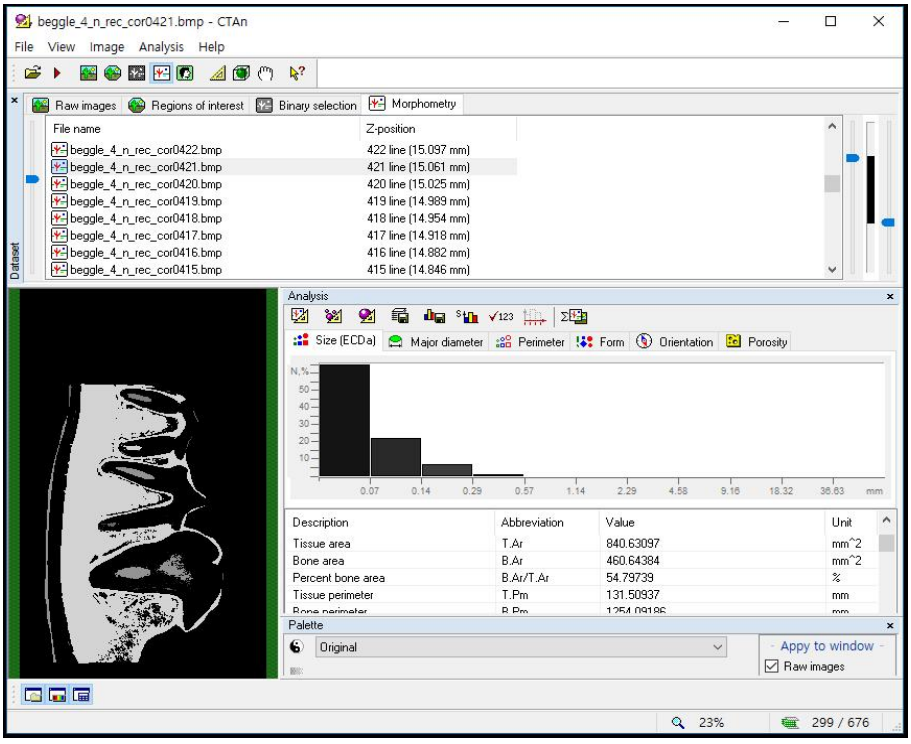

(c)

Figure 2. Obtaining tissue volume and bone volume by defining regions of interest (ROI) by using left mandible (control side) specimen of beagle ID 4 in micro CT analyzing software (CT-Analyser, ver 1.16.4, SkyScan, Kontich, Belgium). (a) Raw images were loaded. (b) Definition of ROI including 2 premolars and one molar teeth was performed manually. (c) After the binary selection using Otsu's algorithm, the color of the selected bone areas is inversely contrasted.

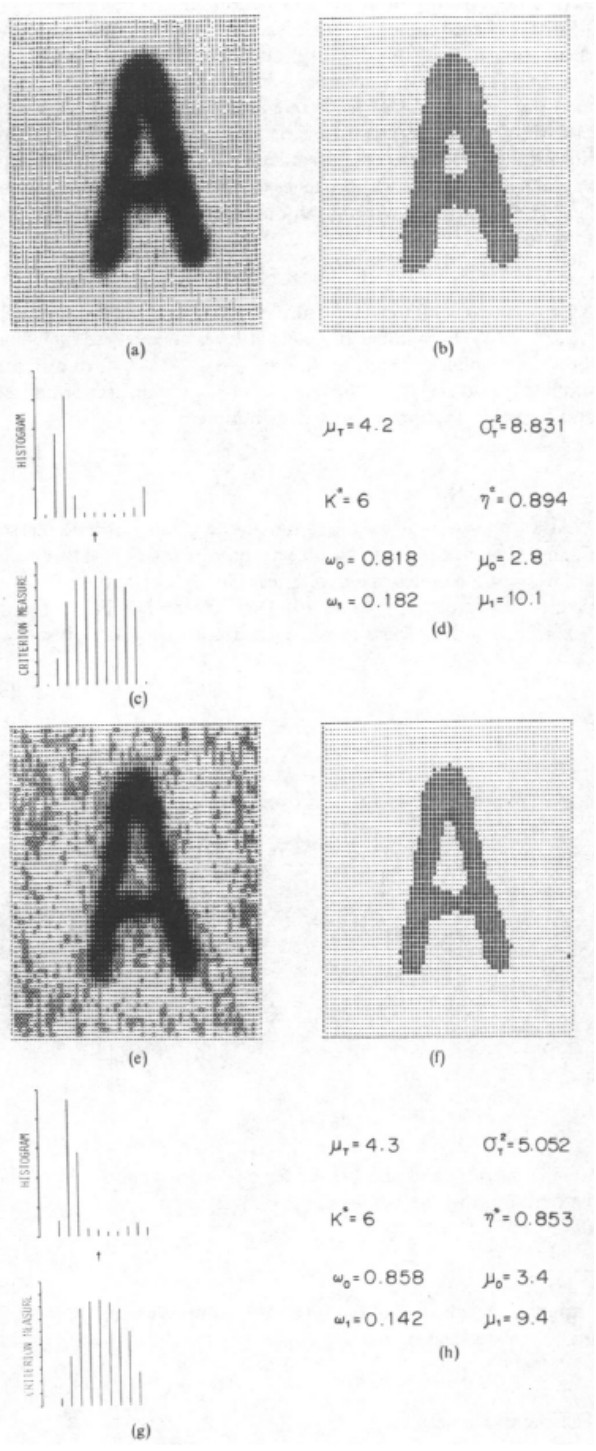

Figure 3. An example showing how binary selection was worked according to the Otsu's algorithm by processing the shape of alphabet 'A' from its background. Picture was adopted from the Otsu's study. [31)]

4. Histological evaluation

Histology was performed after the microCT analysis. Samples were 4% paraformaldehyde fixed and 14% EDTA decalcified for 48 hours, then embedded into paraffin blocks. Samples were sectioned and stained with hematoxylin and eosin (H&E) and Masson Trichrome staining (MT) to visualize bone morphology at the fracture site, device–tissue interface, and within areas of newly formed bone. Local response and biocompatibility were also evaluated.

Results

1. Pre-clinical evaluation

Subcutaneous gas pocket formation was not detected in all animals. Only one beagle (ID 2) developed subcutaneous gas pockets over the implant site, which were simply removed with a sterile syringe without causing infection or interference with healing as shown in Figure 3 (b). In beagle 2, pockets consisted of gas without additional blood or fluid. Gas pocket formation was observed in 3 days post-operative. Subcutaneous gas pocket formation suggests initial evidence of Mg degradation. Additionally, two beagles (ID 1,3) showed hematoma in 3 days post-operative which were removed through a sterile syringe in the same way. (Table 4.)

Otherwise, all beagles didn't show specific postoperative findings and underwent uneventful healing process. All devices were well tolerated by the animals. Immediately following surgery, animals resumed normal jaw movement and general behavior, including chewing, barking and breathing. Overall, biodegradable magnesium devices did not cause any adverse health events.

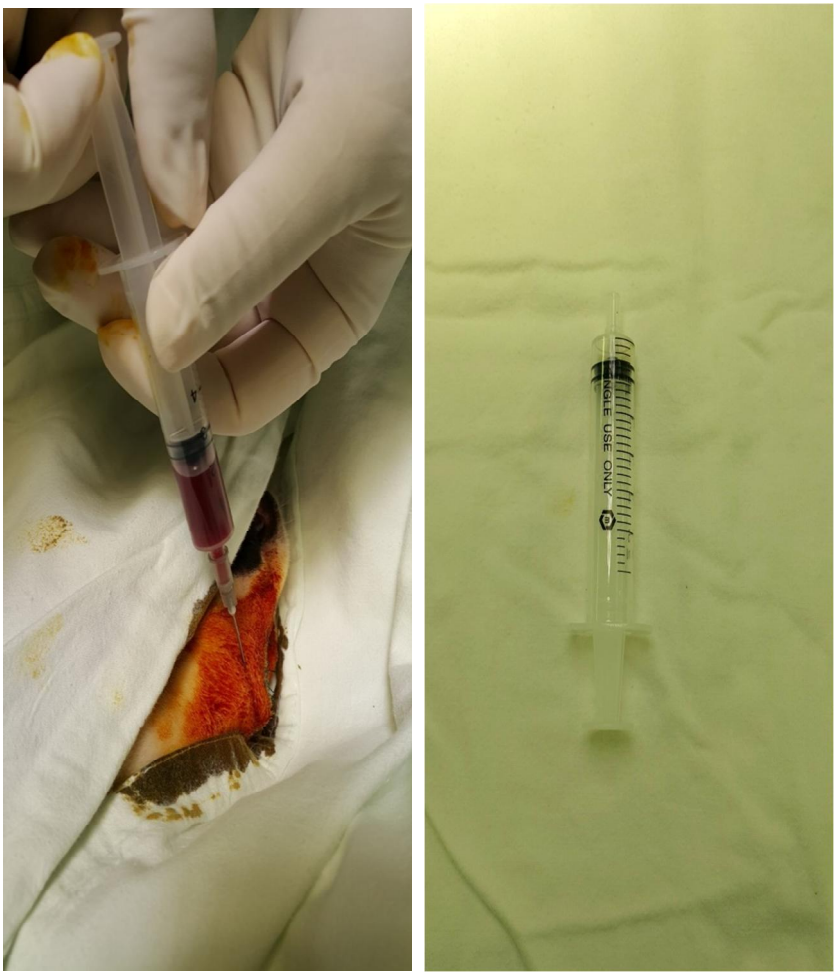

(a) (b)

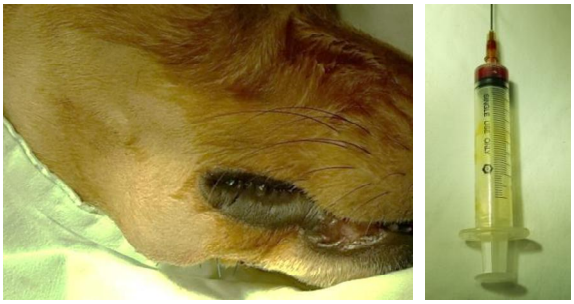

(c) (d)

Figure 4. Hematoma and gas formation in postoperative 3 days (a) Removing hematoma in beagle 1 (b) Removed gas in Beagle 2 (c & d) Swelling of mandible and removed hematoma in beagle 3

Table 4. Post-operative findings of six beagle dogs during the wound healing period.

Beagle ID	Gas pocket formation	Hematoma	Other adverse events
1	No	Yes (3ml)	No
2	Yes (1ml)	No	No
3	No	Yes (1ml)	No
4	No	No	No
5	No	No	No
6	No	No	No

2. Radiographical evaluation

Representative sliced CT images and reconstructed 3D images at 1,4,8,12,16,28 weeks postoperatively were depicted in figure 5. and figure 6. The mandibular bone fractures and the holes on the right mandible were still obvious until 4 weeks and became unclear from 8 weeks with the presence of blurry signs of bone callus, which became continuous bone tissues filling in the gap of the fracture area at 12 weeks postoperatively as shown in figure 6.

Gradual degradation of magnesium plate accompanying local gas generation and new bone formations were observed throughout the post-operative period as shown in figure 5.

Ongoing device degradation in post-operative 5 month from the specimen of sacrificed beagle ID 3 was shown in figure 7.

The total calculated values including tissue and bone volume as previously mentioned are shown in Table 5. and summarized in Table 6.

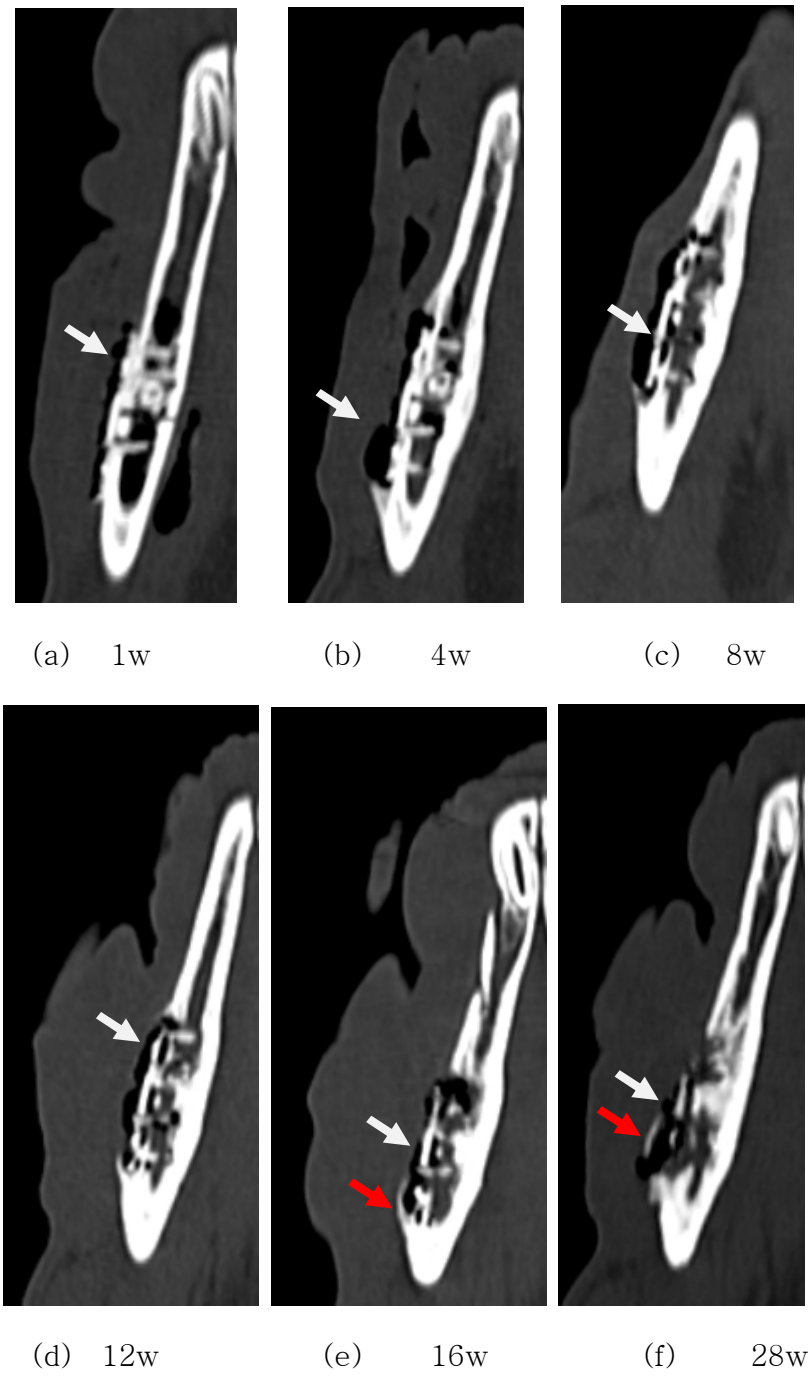

Figure 5. Computed tomography 2-dimensional view of magnesium plate and screw in the right mandible of beagle 1 showing local gas generation (white arrows) in ongoing device degradation and new bone formation (in (f), red arrow).

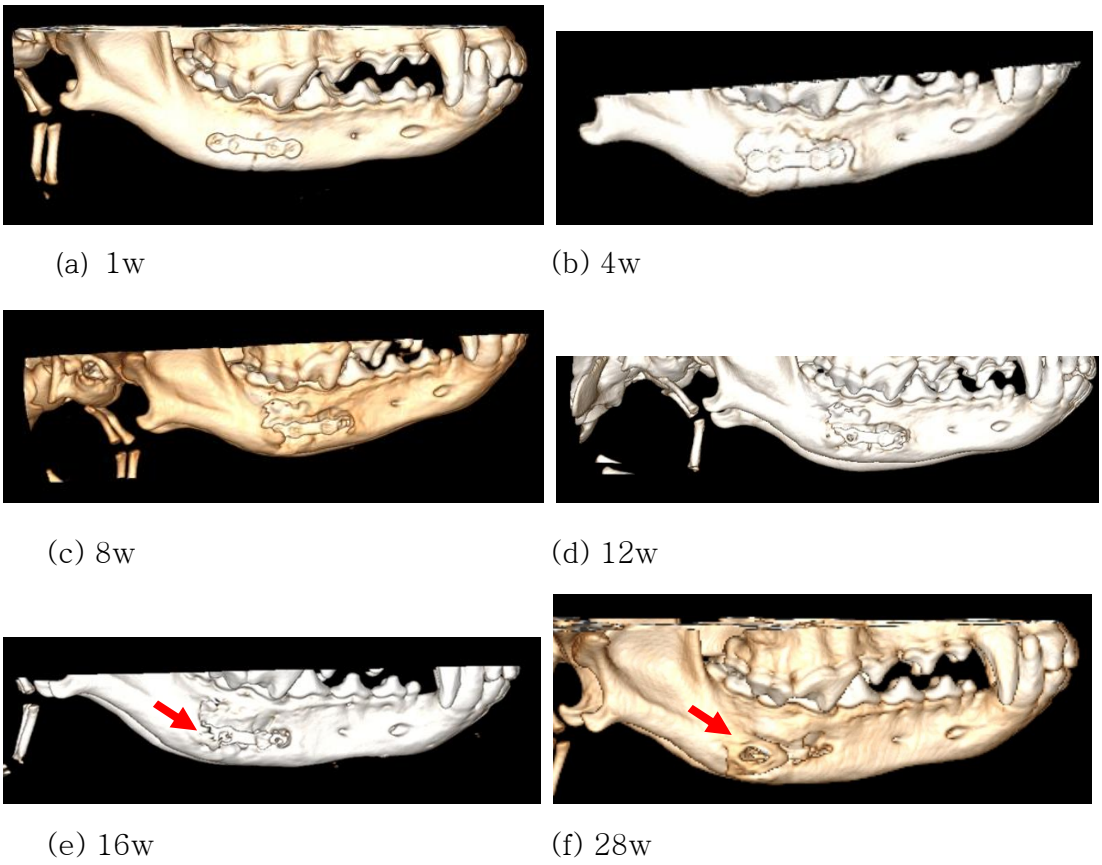

Figure 6. Computed tomography 3-dimensional rendering of magnesium plate and screw in the right mandible of beagle 1 showing ongoing device degradation and new bone formation (in (e) and (f), red arrow).

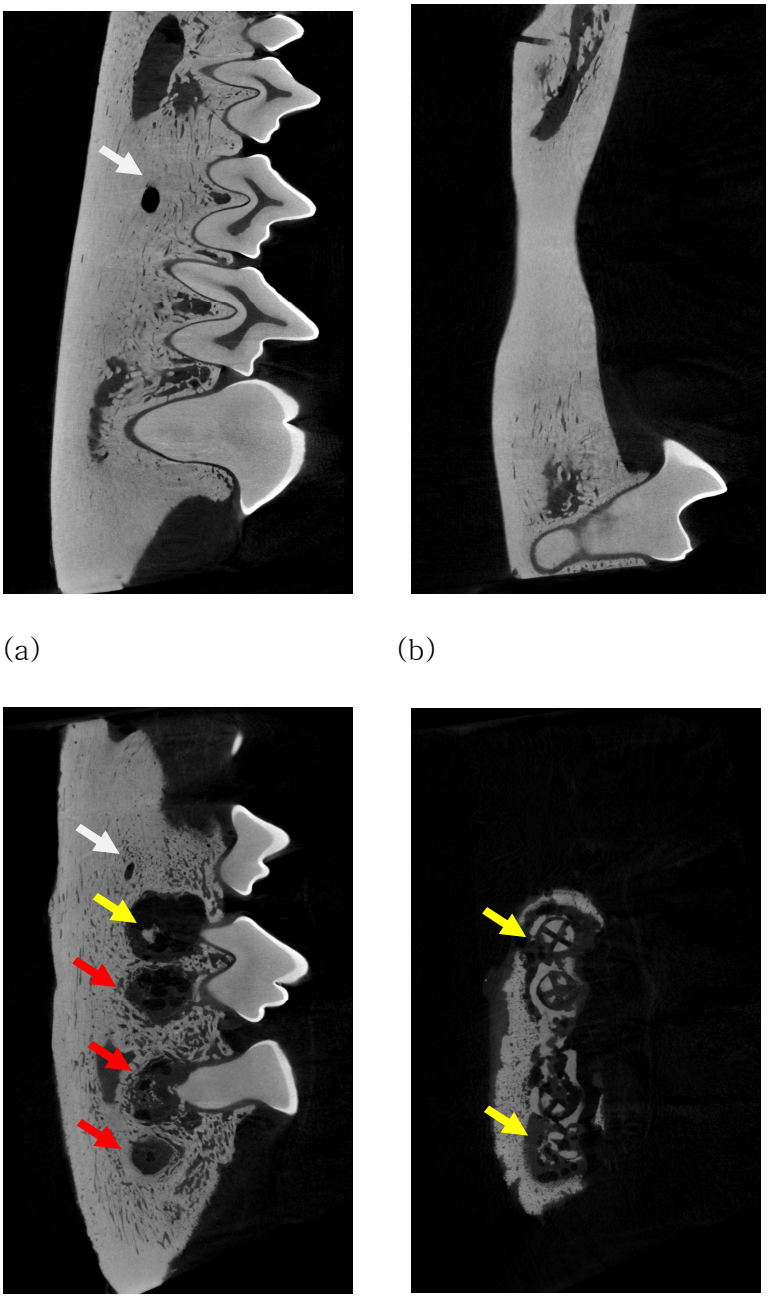

(a) (b)

(c) (d)

Figure. 7. Selected left and right sectional microCT images of beagle 3 which is sacrificed 5 months after the operation. (a) and (b) : Left; (c) and (d) : Right. Mental foramens as normal anatomical structure (white arrow), bone defects around device (red arrow) and ongoing device degradations (yellow arrow) were shown.

Table 5. The total calculated values including tissue and bone volume in mandible (Mn.) specimen of three beagle dogs (a) Left (control side, Lt.) Mn. and right (operated side, Rt.) Mn. of beagle no. 3 (a) Lt. Mn. and Rt. Mn. of beagle no. 4 (a) Lt. Mn. and Rt. Mn. of beagle no. 6

(a)

Description	Abbreviation	Value (Lt.)	Value (Rt.)	Unit
Number of layers		301	431	
Lower vertical position		8.58584	5.72389	mm
Upper vertical position		19.31814	21.10686	mm
Pixel size		35.77434	35.77434	um
Lower grey threshold		0	0	
Upper grey threshold		127	127	
Tissue volume	TV	8026.0181	10278.756	mm^3
Bone volume	BV	3929.2385	8098.1128	mm^3
Percent bone volume	BV/TV	48.95626	78.78495	%
Tissue surface	TS	4014.1469	4287.3685	mm^2
Bone surface	BS	22393.158	24157.81	mm^2
Intersection surface	i.S	3164.7972	3613.5937	mm^2
Bone surface / volume ratio	BS/BV	5.69911	2.98314	1/mm
Bone surface density	BS/TV	2.79007	2.35027	1/mm
Trabecular pattern factor	Tb.Pf	-3.61218	-10.61061	1/mm
Centroid (x)	Crd.X	16.24695	16.82281	mm
Centroid (y)	Crd.Y	21.74343	23.69459	mm
Centroid (z)	Crd.Z	14.17	13.57474	mm

Moment of inertia (x)	MMI(x)	636666.48	1227514.1	mm^5
Moment of inertia (y)	MMI(y)	179108.78	392271.49	mm^5
Moment of inertia (z)	MMI(z)	777215.41	1454886	mm^5
Polar moment of inertia	MMI(polar)	796495.33	1537335.8	mm^5
Radius of gyration (x)	Gr.R(x)	12.71885	12.31724	mm
Radius of gyration (y)	Gr.R(y)	6.74606	6.96296	mm
Radius of gyration (z)	Gr.R(z)	14.05279	13.40957	mm
Polar radius of gyration	Gr.R(polar)	14.22603	13.7843	mm
Product of inertia (xy)	Pr.In(xy)	-3098.565	-100615.8	mm^5
Product of inertia (xz)	Pr.In(xz)	6629.1667	48634.637	mm^5
Product of inertia (yz)	Pr.In(yz)	25203.04	-60827.44	mm^5
Total orientation (theta)	T.Or(theta)	87.59537	86.48481	
Total orientation (phi)	T.Or(phi)	90.35231	276.94061	

(b)

Description	Abbreviation	Value (Lt.)	Value (Rt.)	Unit
Number of layers		299	451	
Lower vertical position		7.9419	7.15487	mm
Upper vertical position		18.60265	23.25332	mm
Pixel size		35.77434	35.77434	um
Lower grey threshold		0	0	
Upper grey threshold		127	127	
Tissue volume	TV	6336.585	8554.292	mm^3
Bone volume	BV	2979.979	7101.305	mm^3
Percent bone volume	BV/TV	47.02816	83.01452	%

Tissue surface	TS	3625.68	4305.747	mm^2
Bone surface	BS	17567.94	17939.96	mm^2
Intersection surface	i.S	2528.018	3370.947	mm^2
Bone surface / volume ratio	BS/BV	5.89532	2.52629	1/mm
Bone surface density	BS/TV	2.77246	2.09719	1/mm
Trabecular pattern factor	Tb.Pf	-3.41843	-12.39409	1/mm
Centroid (x)	Crd.X	14.91718	12.55135	mm
Centroid (y)	Crd.Y	20.73163	30.11583	mm
Centroid (z)	Crd.Z	14.23348	13.739	mm
Moment of inertia (x)	MMI(x)	407586.6	1138463	mm^5
Moment of inertia (y)	MMI(y)	106750.8	308005.2	mm^5
Moment of inertia (z)	MMI(z)	482971.5	1285835	mm^5
Polar moment of inertia	MMI(polar)	498654.5	1366151	mm^5
Radius of gyration (x)	Gr.R(x)	11.6871	12.66866	mm
Radius of gyration (y)	Gr.R(y)	5.98112	6.58947	mm
Radius of gyration (z)	Gr.R(z)	12.72206	13.46368	mm
Polar radius of gyration	Gr.R(polar)	12.92697	13.8778	mm
Product of inertia (xy)	Pr.In(xy)	-11570.8	-66915.86	mm^5
Product of inertia (xz)	Pr.In(xz)	-4206.4	42556.74	mm^5
Product of inertia (yz)	Pr.In(yz)	34360.15	-149682.8	mm^5
Total orientation (theta)	T.Or(theta)	84.80982	81.36849	
Total orientation (phi)	T.Or(phi)	92.24863	274.884	

(c)

Description	Abbreviation	Value (Lt.)	Value (Rt.)	Unit
Number of layers		805	781	
Lower vertical position		7.15487	6.08164	mm
Upper vertical position		35.91743	33.98562	mm
Pixel size		35.77434	35.77434	um
Lower grey threshold		0	0	
Upper grey threshold		30	30	
Tissue volume	TV	6893.224	7980.6036	mm^3
Bone volume	BV	892.2714	1101.3626	mm^3
Percent bone volume	BV/TV	12.94418	13.80049	%
Tissue surface	TS	3567.019	3624.7432	mm^2
Bone surface	BS	16614.64	21013.268	mm^2
Intersection surface	i.S	1755.152	1955.4043	mm^2
Bone surface / volume ratio	BS/BV	18.62061	19.07934	1/mm
Bone surface density	BS/TV	2.41029	2.63304	1/mm
Trabecular pattern factor	Tb.Pf	-0.10784	0.7575	1/mm
Centroid (x)	Crd.X	37.3857	40.65543	mm
Centroid (y)	Crd.Y	29.60404	28.46438	mm
Centroid (z)	Crd.Z	23.9524	21.2493	mm
Moment of inertia (x)	MMI(x)	55572.11	92340.642	mm^5
Moment of inertia (y)	MMI(y)	179811.1	206575.09	mm^5
Moment of inertia (z)	MMI(z)	159654.9	198977.7	mm^5
Polar moment of inertia	MMI(polar)	197519.1	248946.72	mm^5
Radius of gyration (x)	Gr.R(x)	7.84212	9.08499	mm
Radius of gyration (y)	Gr.R(y)	14.10631	13.58835	mm

Radius of gyration (z)	Gr.R(z)	13.29219	13.33614	mm
Polar radius of gyration	Gr.R(polar)	14.78461	14.91699	mm
Product of inertia (xy)	Pr.In(xy)	-38900.4	-63372.21	mm^5
Product of inertia (xz)	Pr.In(xz)	1199.707	10541.159	mm^5
Product of inertia (yz)	Pr.In(yz)	-3943.56	9261.2957	mm^5
Total orientation (theta)	T.Or(theta)	88.8853	87.496	
Total orientation (phi)	T.Or(phi)	343.9459	336.20103	

Table 6. Summarized tissue volumes and bone volumes of the bony segment according to the microCT analysis.

ID	Area	TV	BV	BV/TV
3	Lt.Mn.	8026	3929	49.0
	Rt.Mn.	10279	8098	78.8
4	Lt.Mn.	6337	2980	47.0
	Rt.Mn.	8554	7101	83.0
6	Lt.Mn.	6893	892	12.9
	Rt.Mn.	7981	1101	13.8

Rt. : Right, Lt. : Left, Mn. : Mandible, TV : Tissue volume [mm^3] , BV : Bone volume [mm^3], BV/TV : Bone volume / Tissue volume [%]

3. Histological evaluation

Long term histological samples were taken from beagle ID 6 which was sacrificed after one year and four months postoperatively
Comparatively, representative images of left and right mandibles are shown in figure 8. and figure 9.

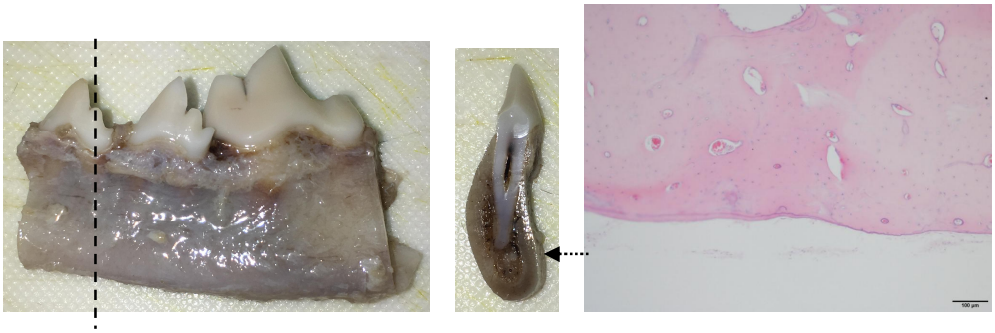

(a) (b) (c)

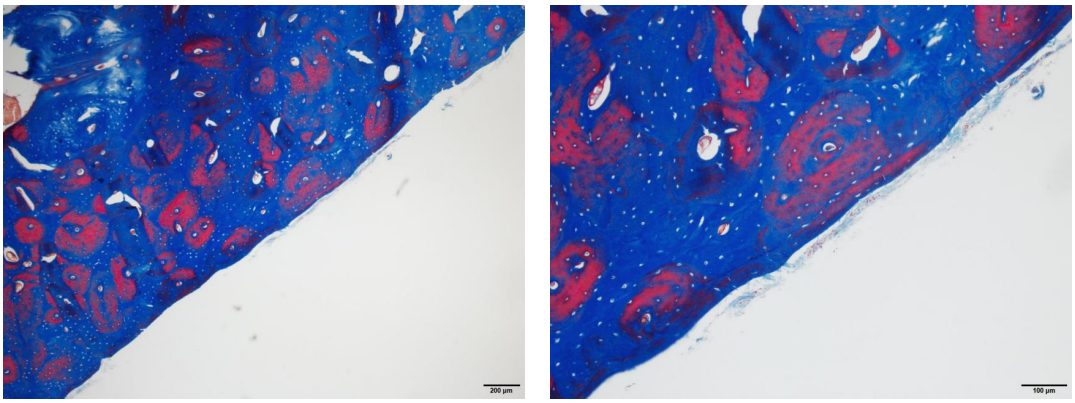

(d) (e)

Figure 8. Histomorphological analysis of left (control side) mandibles of beagle ID 6 which was sacrificed after one year and four months postoperatively. (a) normal appearance of the left mandible. (b) slim and curved surface morphology of the sliced specimen (c) matured lamellar bony structures were shown (Hematoxylin and eosin staining, × 100) (d) (Masson trichrome staining, × 40) (e) (Masson trichrome staining, × 100)

Dotted line : the sliced surface, dotted arrow : the observed area, Blue stain : the expression of collagen.

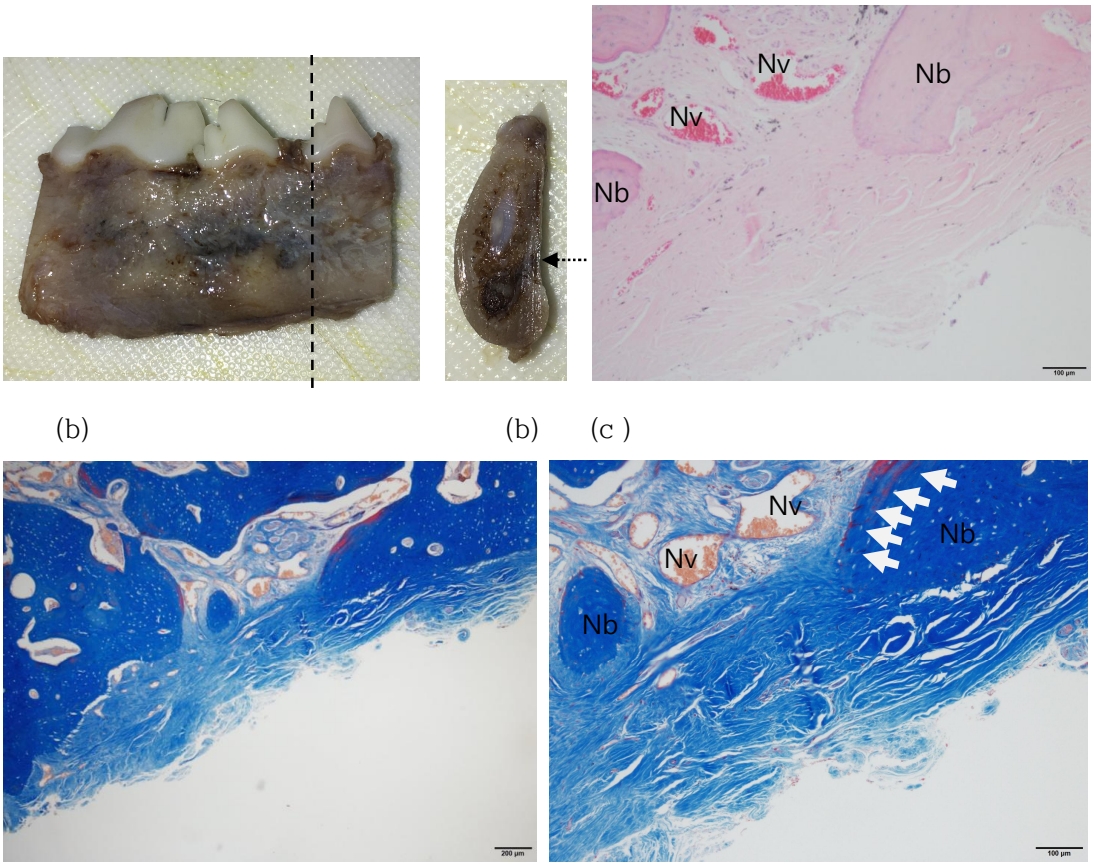

(b) (b) (c) (d) (e)

Figure 9. Histomorphological analysis of right mandibles of beagle ID 6 which was sacrificed after one year and four months postoperatively (a) the right mandible shows black pigmentation around the previous surgical area, (b) thick and flat surface morphology of the sliced specimen (c) newly formed bony structures and irregular periosteal membrane artifact due to its fibrous proliferation were shown. (Hematoxylin and eosin staining, × 100) (d) (Masson trichrome staining, × 40) (e) (Masson trichrome staining, × 100)

Dotted line : the sliced surface, dotted arrow : the observed area, Nb : newly formed bone, Nv :newly formed blood vessels, Blue stain : the expression of collagen, White arrows : lines of osteoblasts.

Discussion

In this study, we investigated the safety and efficacy of biodegradable magnesium alloy plates and screws in a beagle model of a mandible fracture. Previously, our group conducted a series of pilot studies evaluating the biological effect of Mg plates and screws in rabbit model. These studies found that new bone is formed around the degrading Mg devices, suggesting a relationship between Mg degradation and bone formation. To further explore the effect of Mg on fracture healing and bone formation in human, we have performed a thorough investigation of biodegradable magnesium fixation plates and screws in dogs. As previously mentioned, beagles, in which the masticatory and oral conditions were similar those of humans, were routinely selected as an experiment related to dentistry such as periodontics, orthodontics and CMF surgery. [27-29] Especially, the beagle's bite force is approximately 500 N when using the masseter muscle, being comparable to that in humans. [32,33]

In the pre-clinical evaluation, two dogs (ID 1,3) developed hematoma and only one dog (ID 2) formed gas pocket. Hematoma is considered the least complication of surgical intervention. After removing it, two dogs (ID 1,3) underwent normal healing process. The gas pocket was observed in only one dog, indicating that most gas released during device degradation was efficiently cleared from the implant site in other five dogs. It is suggested that gas pocket formation is associated with Mg degradation in numerous study groups including our group. [15,34] The observed gas accumulation did not interrupt bony healing process or cause harm to the surrounding tissue health. However, gas formation in vivo had been a critical issue in study of magnesium plates and screws. Various factors contribute to the process of hydrogen gas release, including the content of magnesium, osmolality and

acidity of the neighboring tissue, and manufacturing method. [4,35,36] Gas formation can be also serious problem in the esthetic point of view. Reducing gas pocket formation is required for clinical translation. Without the proper management of this issue, it is not recommended to apply such gas forming product in human facial bone.

In radiographical evaluation, as we mentioned above, CT imagings were performed 5 times at 4 weeks interval (1, 4, 8, 12, 16 weeks) immediately after implantation. During the observation period, all animals showed ongoing device corrosion, uneventful healing process of mandible fracture and, most importantly, *de novo* bone formation around the inserted device. As shown in Fig. 5 and Fig. 6, new bone deposition over biodegradable magnesium plate was observed radiographically. In 12 and 16 weeks postoperatively, it became so obvious that new bone grown over biodegradable plate was detected grossly.

Since our study began, four of the six beagles have been sacrificed. As shown in Table 5., many values including the tissue and bone volume were derived from comparative analysis in right and left mandible. We summarized tissue and bone volumes out of total values in Table 6. The beagles ID 3,4 were sacrifice after 5 months and ID 6 was devoted after one year and four months postoperatively. We couldn't process the microCT data of beagle ID 5 because its radiographic orientation was not properly aligned. Currently, volumetric analysis of three animals are possible.

Both tissue volume and bone volume/ tissue volume (BV/TV, bone/tissue ratio, [%]) were observed greater in right side than left side in all animals. Especially, Beagle 3 and 4 underwent plate implantation operation 5 months ago, had plate which was on degradation phase on the moment of sacrifice.

After the sacrifice, mandible was analyzed through the microCT and there was a huge bony defect area around the degrading device as shown in figure 7. It would have increased some radiolucent area. Despite of it, BV/TV of two Rt. Mn. Specimen (78.8% and 83.0%) was highly enough than those of Lt. Mn. (49.0% and 47.0%). These results support the fact the magnesium device facilitates mineral deposition around it. However, in beagle ID 6 which was sacrificed one year and four months after operation, the difference between BV/TV of Rt. Mn. (13.8%) and Lt. Mn. (12.9%) was not so significant as shown in ID 3 and 4. However, all values (TV, BV, BV/TV) of Rt. Mn. were higher than that of Lt. Mn. These provide clear evidences that biodegradable magnesium plates contributed hypertrophic bony growth and additional mineral deposition around the surgical area in the long-term observation.

Histomorphometrically, in the sliced sample in beagle ID 1 which sacrificed after one year and four months postoperatively, thick and flat surface morphology was observed in the right mandible (operated side) than slim and curved surface morphology in the left mandible (control side). The H&E and Masson Trichrome stained specimen demonstrated the formation of new vessel and bone. It shows the ability of biodegradable magnesium plates to provide physiological healing and long-term remodeling in a loaded fracture environment that is analogous to human. More importantly, this reflects an advantage of Mg alloys over resorbable polymer devices like poly-l-lactide plate system, which are often inappropriate for the dynamic and load bearing environment.

To improve characteristics of magnesium plate, a wide array of attempts had been tried by numerous study groups such as surface modification, mechanical alloying.[15,37] Recently many advancements were reported in term of corrosion resistance, mechanical properties and biological performance of

magnesium product by alloying zirconium, hydroxyapatite coating and rhBMP-2 application. [38-40)]

Numerous studies have reported bone response around magnesium implant. [16,18,25,36)] One study group observed that newly formed bone was primarily in the periosteal and endosteal areas of bones with implanted magnesium alloys using flouroscopic images of cross-sections as shown in Figure 10.[16)] They also incorporated element mapping analysis such as calcium and phosphorus and found that abundant calcium and phosphorus were detected around the surface of magnesium implant in Figure 11. This corresponds to our finding that increased tissue volume and bone/tissue ratio were observed in all sacrificed animals. As these results suggest, magnesium is an osteoconductive metal.

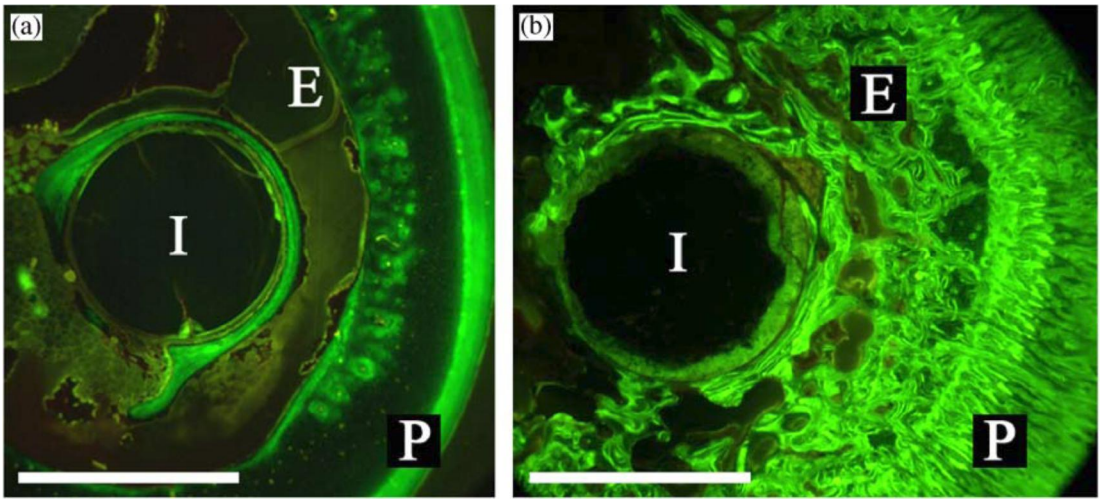

Figure 10. Flouroscopic images of cross-sections of a degradable polymer (a) and a magnesium rod (b) performed 10mm below the trochanter major in a guinea pig femur. Both specimens were harvested 18 weeks postoperatively. In vivo staining of newly formed bone by calcein green. Bar=1.5mm; I=implant residual; P=periosteal bone formation; E=endosteal bone formation. Adopted from a study of Witte. F. et. al.

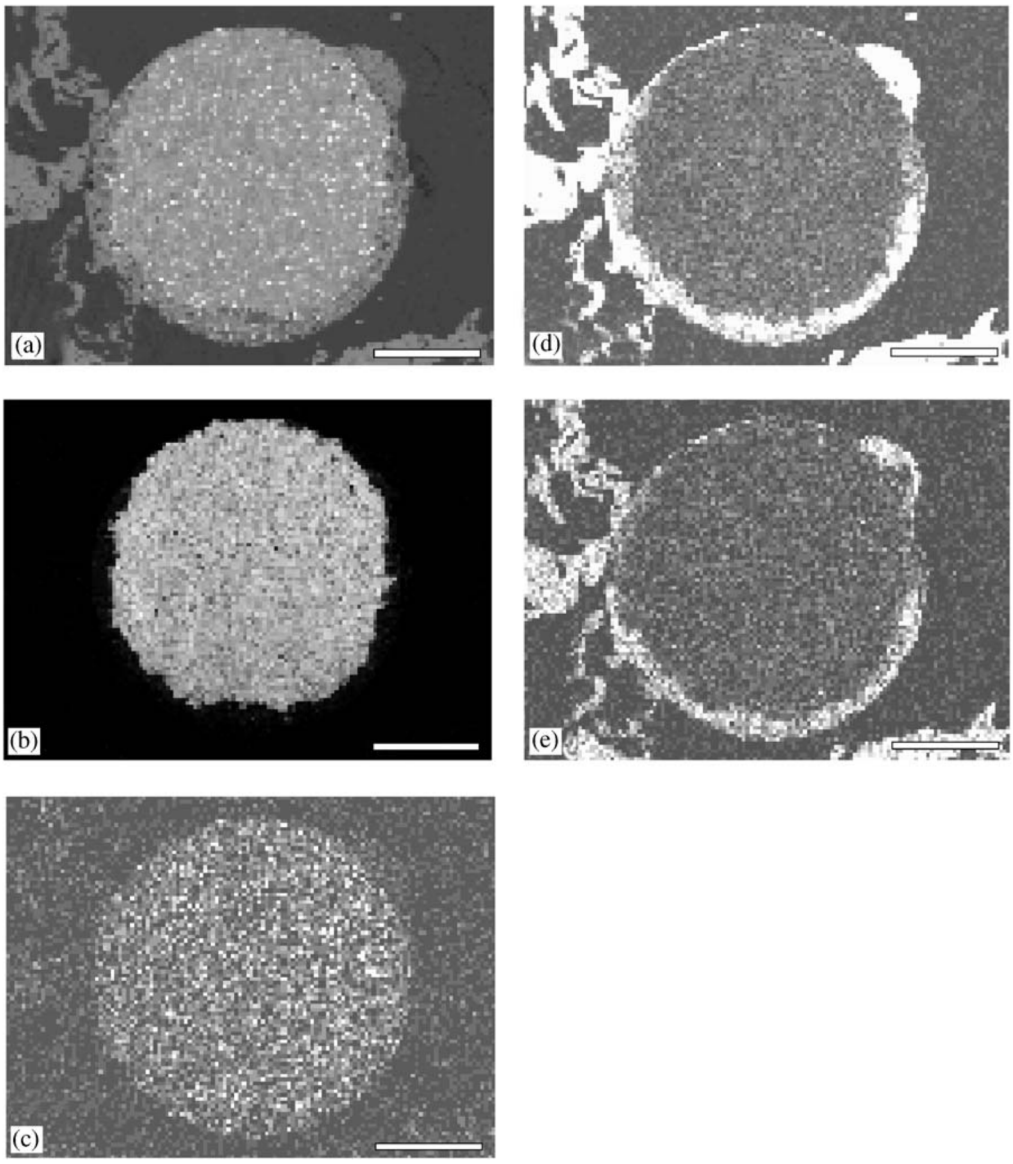

Figure 11. Element mapping analysis on a cross-section of a WE43 magnesium specimen after 6 weeks. (a) back scattered projection, (b) high concentration of magnesium in the non-degraded implant, (c) homogeneous distribution of neodymium in corrosion layer and implant, (d) calcium is mainly located in the surrounding bone and in the corrosion layer, (e) the phosphorous distribution is analogue to the calcium distribution in the corrosion layer. Adopted from a study of Witte. F. et. al.

Historically, dental professions have met many different moments that bone volume required to be increased such as periodontics, orthodontics and CMF implant surgery.[29,41-43] So, after the establishment of clinical safety and efficacy, it might be a good idea to use this material as vertical and horizontal reconstructive surgery of alveolar bone. There have been many attempts to use growth factors to increase vertical and horizontal dimension of alveolar bone in clinical dentistry as shown in Table 7. There are many growth factors studied, but Platelet-rich plasma (PRP) and BMP is commercially available now. PRP is a volume of autogenous plasma that has a platelet concentration above baseline (1 million platelets/mL versus normal average of 200,000 platelets/mL). Typically 20 to 60 mL of blood is drawn from the patient to produce a sufficient PRP volume for dental use. It requires additional invasive procedure for the autologous blood acquisition. For this reason, it is not so widely used in clinical dentistry. The reconstructive methods that can reliably restore bone with the characteristics necessary for maintaining osseointegrated implants could be classified into autogenous cancellous bone grafts, distraction histiogenesis alone or with graft supplementation and the use of rhBMP-2. [44] In actual practice, the first and the last option are frequently used because distraction histiogenesis device is too burdensome to install and be utilized widely in clinical environment.

Table 7. Growth factors currently used for clinical dentistry.

Growth Factors	Clinically available
Platelet-derived growth factor (PDGF)	No
Fibroblast growth factor (FGF)	No
Transforming growth factor (TGF)	No
Insulinlike growth factor (IGF)	No
Platelet-rich plasma (PRP)	Yes
Bone morphogenic proteins (BMP)	Yes

PRP contains PDGF aa, PDGF bb, PDGF Fab, TGF-b1, TGF-b2, VEGF, Epithelial growth factor.

PDGF, Platelet-derived growth factor; TGF, transforming growth factor; VEGF, vascular endothelial growth factor.

Autologous bone grafts have been performed to augment alveolar bone but there is a risk of nerve injury and pathological fracture due to donor site morbidity. [45,46] The bone graft material using rhBMP-2 with collagen sponge, synthetic HA / β-TCP also have been used with good reliability. [47-49] There is no donor site morbidity with using these materials, but it is difficult to obtain initial fixation stability which is necessary for callus formation.

In this study, we obtained proper initial fixation with biodegradable magnesium plate that have osteoconductivity and found active new bone formation that persisted even after 1 year and 4 months. To the best of author's knowledge, it could be useful to use this material in alveolar bony ridge augmentation procedure since plate and screw devices have superior initial fixation quality than particle or membrane material.

At this moment, studies on the specific mechanism of bone apposition and tissue growth are still far away. The development, performance and integration with bone tissue of porous magnesium-based implants are also topics requiring further investigation.

The limitation of this study could be relatively small sample size (n=6) and postoperative management. Unlike in humans, postoperative care, such as sterile wound environment, regulation of the diet, and behavioral control, were not possible in an animal study. Additional clinical studies are recommended to be performed in future.

Conclusion

In the present study we assessed the safety and efficacy of degradable biodegradable magnesium fixation plates and screws in a loaded beagle mandible fracture model. We have demonstrated that Mg device degradation does not inhibit fracture healing and enhances bone formation around the devices. Furthermore, we observed de novo bone formation above the devices, suggesting osteoconductive property of Mg plate systems. These data support the potential use of Mg alloys as fracture fixation devices.

References

1. Marcus SE, Drury TF, Brown LJ, Zion GR. Tooth retention and tooth loss in the permanent dentition of adults: United States, 1988-1991. J Dent Res 1996;75 Spec No:684-695.

2. Nissan J, Kolerman R, Chaushu L, Vered M, Naishlos S, Chaushu G. Age-related new bone formation following the use of cancellous bone-block allografts for reconstruction of atrophic alveolar ridges. Clin Implant Dent Relat Res 2018;20:4-8.

3. Stevens B, Yang Y, Mohandas A, Stucker B, Nguyen KT. A review of materials, fabrication methods, and strategies used to enhance bone regeneration in engineered bone tissues. Journal of Biomedical Materials Research Part B: Applied Biomaterials 2008;85B:573-582.

4. Staiger MP, Pietak AM, Huadmai J, Dias G. Magnesium and its alloys as orthopedic biomaterials: a review. Biomaterials 2006;27:1728-1734.

5. Pietak A, Mahoney P, Dias GJ, Staiger MP. Bone-like matrix formation on magnesium and magnesium alloys. J Mater Sci Mater Med 2008;19:407-415.

6. Rokkanen PU, Bostman O, Hirvensalo E, Makela EA, Partio EK, Patiala H et al. Bioabsorbable fixation in orthopaedic surgery and traumatology. Biomaterials 2000;21:2607-2613.

7. Sukegawa S, Kanno T, Manabe Y, Matsumoto K, Sukegawa-Takahashi Y, Masui M et al. Biomechanical Loading Evaluation of Unsintered Hydroxyapatite/poly-l-lactide Plate System in Bilateral Sagittal Split Ramus Osteotomy. Materials (Basel) 2017;10.

8. Choi SH, Lee JH. Absorbable Plate-Related Infection after Facial Bone Fracture Reduction. Arch Craniofac Surg 2016;17:1-4.

9. Wolff M, Luczak M, Schaper JG, Wiese B, Dahms M, Ebel T et al. In vitro biodegradation testing of Mg-alloy EZK400 and manufacturing of implant prototypes using PM (powder metallurgy) methods. Bioact Mater 2018;3:213-217.

10. Waris E, Ashammakhi N, Kaarela O, Raatikainen T, Vasenius J. Use of

bioabsorbable osteofixation devices in the hand. J Hand Surg Br 2004;29:590-598.
11. Peltoniemi H, Ashammakhi N, Kontio R, Waris T, Salo A, Lindqvist C et al. The use of bioabsorbable osteofixation devices in craniomaxillofacial surgery. Oral Surg Oral Med Oral Pathol Oral Radiol Endod 2002;94:5-14.
12. Nha KW, Oh SM, Ha YW, Nikumbha VP, Seo JH, Oh MJ et al. A Retrospective Comparison of Union Rates After Open Wedge High Tibial Osteotomies With and Without Synthetic Bone Grafts (Hydroxyapatite and beta-tricalciumphosphate) at 2 Years. Arthroscopy 2018;34:2621-2630.
13. Buser Z, Brodke DS, Youssef JA, Meisel HJ, Myhre SL, Hashimoto R et al. Synthetic bone graft versus autograft or allograft for spinal fusion: a systematic review. J Neurosurg Spine 2016;25:509-516.
14. Russias J, Saiz E, Nalla RK, Gryn K, Ritchie RO, Tomsia AP. Fabrication and mechanical properties of PLA/HA composites: A study of in vitro degradation. Mater Sci Eng C Biomim Supramol Syst 2006;26:1289-1295.
15. Lim HK, Byun SH, Woo JM, Kim SM, Lee SM, Kim BJ et al. Biocompatibility and Biocorrosion of Hydroxyapatite-Coated Magnesium Plate: Animal Experiment. Materials (Basel) 2017;10.
16. Witte F, Kaese V, Haferkamp H, Switzer E, Meyer-Lindenberg A, Wirth CJ et al. In vivo corrosion of four magnesium alloys and the associated bone response. Biomaterials 2005;26:3557-3563.
17. Li Z, Gu X, Lou S, Zheng Y. The development of binary Mg-Ca alloys for use as biodegradable materials within bone. Biomaterials 2008;29:1329-1344.
18. Witte F, Fischer J, Nellesen J, Crostack HA, Kaese V, Pisch A et al. In vitro and in vivo corrosion measurements of magnesium alloys. Biomaterials 2006;27:1013-1018.
19. Heublein B, Rohde R, Kaese V, Niemeyer M, Hartung W, Haverich A. Biocorrosion of magnesium alloys: a new principle in cardiovascular implant technology? Heart 2003;89:651-656.
20. Saris NE, Mervaala E, Karppanen H, Khawaja JA, Lewenstam A. Magnesium. An update on physiological, clinical and analytical aspects. Clin Chim Acta 2000;294:1-

26.
21. He K, Liu K, Daviglus ML, Morris SJ, Loria CM, Van Horn L et al. Magnesium intake and incidence of metabolic syndrome among young adults. Circulation 2006;113:1675-1682.
22. Chaya A, Yoshizawa S, Verdelis K, Noorani S, Costello BJ, Sfeir C. Fracture healing using degradable magnesium fixation plates and screws. J Oral Maxillofac Surg 2015;73:295-305.
23. Kraus T, Fischerauer SF, Hänzi AC, Uggowitzer PJ, Löffler JF, Weinberg AM. Magnesium alloys for temporary implants in osteosynthesis: In vivo studies of their degradation and interaction with bone. Acta Biomaterialia 2012;8:1230-1238.
24. Willbold E, Kalla K, Bartsch I, Bobe K, Brauneis M, Remennik S et al. Biocompatibility of rapidly solidified magnesium alloy RS66 as a temporary biodegradable metal. Acta Biomaterialia 2013;9:8509-8517.
25. Janning C, Willbold E, Vogt C, Nellesen J, Meyer-Lindenberg A, Windhagen H et al. Magnesium hydroxide temporarily enhancing osteoblast activity and decreasing the osteoclast number in peri-implant bone remodelling. Acta Biomaterialia 2010;6:1861-1868.
26. Yang J, Cui F, Lee I-S, Zhang Y, Yin Q, Xia H et al. In vivo biocompatibility and degradation behavior of Mg alloy coated by calcium phosphate in a rabbit model. Journal of Biomaterials Applications 2012;27:153-164.
27. Matthew IR, Frame JW. Release of metal in vivo from stressed and nonstressed maxillofacial fracture plates and screws. Oral Surg Oral Med Oral Pathol Oral Radiol Endod 2000;90:33-38.
28. Kim S, Herring S, Wang IC, Alcalde R, Mak V, Fu I et al. A comparison of miniplates and teeth for orthodontic anchorage. Am J Orthod Dentofacial Orthop 2008;133:189.e181-189.
29. Ikawa T, Akizuki T, Matsuura T, Hoshi S, Ammar SA, Kinoshita A et al. Ridge Preservation After Tooth Extraction With Buccal Bone Plate Deficiency Using Tunnel Structured beta-Tricalcium Phosphate Blocks: A 2-Month Histologic Pilot Study in

Beagle Dogs. J Periodontol 2016;87:175-183.
30. Clark JD, Gebhart GF, Gonder JC, Keeling ME, Kohn DF. Special Report: The 1996 Guide for the Care and Use of Laboratory Animals. Ilar j 1997;38:41-48.
31. Otsu N. A Threshold Selection Method from Gray-Level Histograms. IEEE Transactions on Systems, Man, and Cybernetics 1979;9:62-66.
32. Ström D, Holm S. Bite-force development, metabolic and circulatory response to electrical stimulation in the canine and porcine masseter muscles. Archives of Oral Biology 1992;37:997-1006.
33. Christiansen P, Wroe S. BITE FORCES AND EVOLUTIONARY ADAPTATIONS TO FEEDING ECOLOGY IN CARNIVORES. Ecology 2007;88:347-358.
34. Schaller B, Saulacic N, Beck S, Imwinkelried T, Liu EWY, Nakahara K et al. Osteosynthesis of partial rib osteotomy in a miniature pig model using human standard-sized magnesium plate/screw systems: Effect of cyclic deformation on implant integrity and bone healing. J Craniomaxillofac Surg 2017;45:862-871.
35. Cha PR, Han HS, Yang GF, Kim YC, Hong KH, Lee SC et al. Biodegradability engineering of biodegradable Mg alloys: tailoring the electrochemical properties and microstructure of constituent phases. Sci Rep 2013;3:2367.
36. Martinez Sanchez AH, Luthringer BJ, Feyerabend F, Willumeit R. Mg and Mg alloys: how comparable are in vitro and in vivo corrosion rates? A review. Acta Biomater 2015;13:16-31.
37. Wolff M, Luczak M, Schaper JG, Wiese B, Dahms M, Ebel T et al. In vitro biodegradation testing of Mg-alloy EZK400 and manufacturing of implant prototypes using PM (powder metallurgy) methods. Bioact Mater 2018;3:213-217.
38. Cheng M, Qiao Y, Wang Q, Qin H, Zhang X, Liu X. Dual ions implantation of zirconium and nitrogen into magnesium alloys for enhanced corrosion resistance, antimicrobial activity and biocompatibility. Colloids Surf B Biointerfaces 2016;148:200-210.
39. Zhang M, Cai S, Zhang F, Xu G, Wang F, Yu N et al. Preparation and corrosion resistance of magnesium phytic acid/hydroxyapatite composite coatings on

biodegradable AZ31 magnesium alloy. J Mater Sci Mater Med 2017;28:82.
40. Jiang Y, Wang B, Jia Z, Lu X, Fang L, Wang K et al. Polydopamine mediated assembly of hydroxyapatite nanoparticles and bone morphogenetic protein-2 on magnesium alloys for enhanced corrosion resistance and bone regeneration. J Biomed Mater Res A 2017;105:2750-2761.
41. Kim A, Kar K, Nowzari H, Ahn K-M, Cha H. Subapical osteotomy to correct dental implant malpositioning and vertical ridge deficiency: A clinical report. The Journal of Prosthetic Dentistry 2012;108:204-208.
42. You KH, Min YS, Baik HS. Treatment of ankylosed maxillary central incisors by segmental osteotomy with autogenous bone graft. Am J Orthod Dentofacial Orthop 2012;141:495-503.
43. AlKudmani H, Al Jasser R, Andreana S. Is Bone Graft or Guided Bone Regeneration Needed When Placing Immediate Dental Implants? A Systematic Review. Implant Dent 2017;26:936-944.
44. Miloro M, Peterson LJ. Peterson's principles of oral and maxillofacial surgery. Shelton, CT: People's Medical Pub. House-USA; 2012.
45. Uckan S, Veziroglu F, Dayangac E. Alveolar distraction osteogenesis versus autogenous onlay bone grafting for alveolar ridge augmentation: Technique, complications, and implant survival rates. Oral Surgery, Oral Medicine, Oral Pathology, Oral Radiology, and Endodontology 2008;106:511-515.
46. Kwon IJ, Lee BH, Eo MY, Kim SM, Lee JH, Lee SK. Pathologic mandibular fracture after biting crab shells following ramal bone graft. Dent Traumatol 2016;32:421-424.
47. Kelly MP, Vaughn OL, Anderson PA. Systematic Review and Meta-Analysis of Recombinant Human Bone Morphogenetic Protein-2 in Localized Alveolar Ridge and Maxillary Sinus Augmentation. J Oral Maxillofac Surg 2016;74:928-939.
48. Huh JB, Lee HJ, Jang JW, Kim MJ, Yun PY, Kim SH et al. Randomized clinical trial on the efficacy of Escherichia coli-derived rhBMP-2 with beta-TCP/HA in extraction socket. J Adv Prosthodont 2011;3:161-165.
49. Herford AS, Boyne PJ. Reconstruction of mandibular continuity defects with bone

morphogenetic protein-2 (rhBMP-2). J Oral Maxillofac Surg 2008;66:616-624.

국문요약

배경

뼈와 관련된 외상은 매우 흔하며 미국에서는 매년 6 백만 건의 골절이 발생한다. 이 골절은 출생 결함, 골다공증, 골수염, MRONJ (턱의 약물 관련 골 괴사) 및 가장 흔한 외상과 같은 다양한 원인에 의해 발생합니다. 인구가 오래되고 의학적으로 손상된 환자의 수가 증가함에 따라 향후 병리학적 골절의 비율이 증가 할 것으로 예상된다. 이러한 이유로 골절 치료는 뼈 조직 공학에서 중요한 임상적 과제이다. 골절 치료는 종종 내고정을 필요로 한다. Plate와 screw는 뼈 조각의 배열과 초기고정에 사용된다. 일반적으로 금속 및 고분자 물질과 같은 내부 골 고정 장치가 사용되어왔다. 티타늄과 같은 금속으로 만든 내부 앵커는 여러가지 장기적인 합병증과 관련이 있으며 제거가 필요할 수 있다. 고분자 물질은 생분해성이며 제거 할 필요는 없지만 금속보다 기계적 품질이 떨어지는 것으로 알려져 있다.

금속 및 흡수성 고분자와는 달리, 생분해성 마그네슘 합금은 강도와 생체적합성면에서 이상적인 재료로 여겨진다. 생체 내에서 마그네슘 합금에 대한 최근의 연구들은 뼈 고정 물질로서의 잠재성을 보여주고 있다.

목적

생분해성 마그네슘 합금 시스템은 티타늄 또는 흡수성 중합체로 제조 된 종래의 플레이트 및 스크류의 대체물로서 개발되었다. 그러나 이전의 연구는 wire 나 screw를 사용한 작은 동물 실험에 국한되었다. 본 연구에서는 인간 표준 크기의 분해성 마그네슘 장치를 비글의 하악골 골절 모델을 사용하여 평가 하였다. 장치 분해, 골절 치유 및 새로운 골 형성이 평가되었다.

방법

이번 연구에서는 생체분해성 CMF용 Plate 제품의 생물학적 안전성/유효성 중대동물을 이용하여 평가하게 된다. 중/대동물중 저작력과 구강내 조건이 사람과 흡사하여 임플란트 및 기타 치아와 관련된 실험으로 일상적으로 선택되는 Beagle 을 사용하게 되었다. 9kg 의 수컷 비글 6마리 하악 우측 하악골을 2등분 한후 골절부위에 생흡수성 마그네슘 Plate 시제품을 식립 후 16주 동안 식립재 주변의 수소 가스 발생량과 속도, 분해 거동을 평가하여 식립하지 않은 좌측과 비교하여 어떠한 차이를 보이는지 확인한다. 구체적인 확인방법으로는 microCT를 식립수술직후 및 4주 간격으로 5회 촬영하는것과 (1,4,8,12,16 weeks), 6개월, 1년반, 3년후에 sacrifice 후 histology를 수행하여 주변 조직 반응(local response)을 확인하여 이식 시험에 대한 생체 적합성을 비교, 평가하고자 한다.

결과

이 연구에서 사용한 plate 시제품은 16주간 CT 촬영 및 희생 후에 시행한 조직학적, 임상적 평가에서 긍정적인 결과로 관찰되었다. 특히 수술부위의 골형성이 대조부위에 비하여 추가적으로 발견되었으며 특이할만한 부작용이 발견되지 않았다. 시제품을 인간에게 적용하기에 앞서 골침착이 대조부위에 비하여 추가적으로 되는 것과 수술 초기의 수소발생을 억제할 수 있는 방법에 대한 추가적인 연구가 필요할 것으로 생각된다.

중심단어 : 흡수성 플레이트, 마그네슘 플레이트, 비글, 생체적합성